

Article

High-Pressure Synthesis, Crystal Structure, and Photoluminescence Properties of β - $\text{Y}_2\text{B}_4\text{O}_9\text{:Eu}^{3+}$

Birgit Fuchs ¹, Franziska Schröder ², Gunter Heymann ¹, Thomas Jüstel ²  and Hubert Huppertz ^{1,*} 

¹ Institut für Allgemeine, Anorganische und Theoretische Chemie, Universität Innsbruck, Innrain 80–82, 6020 Innsbruck, Austria; birgit.fuchs@uibk.ac.at (B.F.); gunter.heyman@uibk.ac.at (G.H.)

² Fachbereich Chemieingenieurwesen, FH Münster, Stegerwaldstraße 39, 48565 Steinfurt, Germany; franziska.schroeder@fh-muenster.de (F.S.); tj@fh-muenster.de (T.J.)

* Correspondence: hubert.huppertz@uibk.ac.at; Fax: +43-(512)-507-57099

Received: 14 October 2019; Accepted: 9 November 2019; Published: 12 November 2019



Abstract: A high-pressure/high-temperature experiment at 7.5 GPa and 1673 K led to the formation of the new compound β - $\text{Y}_2\text{B}_4\text{O}_9$. In contrast to the already known polymorph α - $\text{Y}_2\text{B}_4\text{O}_9$, which crystallizes in the space group $C2/c$, the reported structure could be solved via single-crystal X-ray diffraction in the triclinic space group $P\bar{1}$ (no. 2) and is isotopic to the already known lanthanide borates β - $\text{Dy}_2\text{B}_4\text{O}_9$ and β - $\text{Gd}_2\text{B}_4\text{O}_9$. Furthermore, the photoluminescence of an europium doped sample of β - $\text{Y}_2\text{B}_4\text{O}_9\text{:Eu}^{3+}$ (8%) was investigated.

Keywords: crystal structure; europium; high-pressure chemistry; photoluminescence; yttrium borate

1. Introduction

In the system Y–B–O, only two modifications of YBO_3 [1] (the low-temperature form π - YBO_3 and the high-temperature form μ - YBO_3) and the compound $\text{Y}_{17.33}(\text{BO}_3)_4(\text{B}_2\text{O}_5)_2\text{O}_{16}$ [2] (revised formula of Y_3BO_6) were known until 2016. Through the implementation of high-pressure conditions as an additional reaction parameter, three new compositions β - $\text{Y}(\text{BO}_2)_3$ [3], α - $\text{Y}_2\text{B}_4\text{O}_9$ [4], and YB_7O_{12} [5] could be obtained by our group. As expected, all of the three latter compounds feature boron exclusively in a fourfold coordination by oxygen anions due to the applied high-pressure conditions. The anionic borate networks of these compounds are built up of corner-sharing and, in the case of α - $\text{Y}_2\text{B}_4\text{O}_9$, also of edge-sharing BO_4 tetrahedra. Not only the coordination number of boron is often increased under high-pressure conditions, but also the oxygen atoms can exhibit an increased coordination number, e.g., coordinated by three boron atoms ($\text{O}^{[3]}$), which is the case, for example, in the borates β - $\text{Y}(\text{BO}_2)_3$ and YB_7O_{12} .

In the following, we report on the high-pressure synthesis of β - $\text{Y}_2\text{B}_4\text{O}_9$, a hitherto missing polymorph of α - $\text{Y}_2\text{B}_4\text{O}_9$. In contrast to the α -modification, which was synthesized at 12.3 GPa, the β -phase was obtained at a lower pressure of 7.5 GPa and does still contain planar BO_3 -groups and no edge-sharing BO_4 tetrahedra. Furthermore, β - $\text{Y}_2\text{B}_4\text{O}_9$ is isotopic to the already known compounds β - $\text{Dy}_2\text{B}_4\text{O}_9$ [6] and β - $\text{Gd}_2\text{B}_4\text{O}_9$ [7], which will be discussed in detail.

Rare earth borates have been known for their excellent properties as hosts for luminescent materials. They possess high quantum yields, an exceptional optical damage threshold, and a long lifetime, which makes them highly attractive for practical applications. The orthoborates $(\text{Y,Gd})\text{BO}_3\text{:Eu}^{3+}$ and $\text{YBO}_3\text{:Tb}^{3+}$ are widely used, for example, in plasma display panels [8,9], but also co-doped inorganic phosphors like $\text{YBO}_3\text{:Eu}^{3+}/\text{Tb}^{3+}$ [10] or $\text{YAl}_3(\text{BO}_3)_4\text{:Eu}^{3+}/\text{Tb}^{3+}$ or $\text{Dy}^{3+}/\text{Tm}^{3+}$ [11,12] are applied. Research in this field is ongoing, as a recently published work on the complete solid

solution of α -Y_{1-x}Eu_xB₅O₉ shows [13]. In connection with these findings, we also investigated the photoluminescence properties of a β -Y₂B₄O₉:Eu³⁺ sample.

2. Results and Discussion

2.1. Crystal Structure

β -Y₂B₄O₉ crystallizes in the triclinic space group $P\bar{1}$ with the cell parameters $a = 6.1463(2)$, $b = 6.4053(2)$, $c = 7.4642(2)$ Å, $\alpha = 102.59(2)^\circ$, $\beta = 97.11(2)^\circ$, and $\gamma = 102.46(2)^\circ$. The unit cell ($V = 275.50(2)$ Å³) comprises $Z = 2$ formula units. All the relevant data of the structure refinement are shown in Table 1.

Table 1. Crystal data and structure refinement of β -Y₂B₄O₉.

Empirical Formula	β -Y ₂ B ₄ O ₉
Molar mass, g·mol ⁻¹	365.06
Crystal system	triclinic
Space group	$P\bar{1}$ (no. 2)
Single-crystal data	
T , K	277(2)
Radiation	Mo K α ($\lambda = 71.07$ pm)
a , Å	6.1463(2)
b , Å	6.4053(2)
c , Å	7.4642(2)
α , °	102.59(2)
β , °	97.11(2)
γ , °	102.46(2)
V , Å ³	275.50(2)
Z	2
Calculated density, g·cm ⁻³	4.401
Absorption coeff., mm ⁻¹	20.993
$F(000)$	340
Crystal size, mm ³	0.050 × 0.040 × 0.020
θ range, °	2.8–41.3
Index ranges	$-11 \leq h \leq 11$, $-11 \leq k \leq 11$, $-13 \leq l \leq 13$
Reflections collected	28267
Independent reflections	3675 [$R_{\text{int}} = 0.0398$]
Refinement method	Full-matrix least-squares on F^2
Data/restraints/parameters	3675/0/137
Goodness-of-fit on F^2	1.058
Final $R1/wR2$ indices [$I \geq 2\sigma(I)$]	0.0210/0.0414
Final $R1/wR2$ indices (all data)	0.0286/0.0431
Largest diff. peak/hole, e Å ⁻³	1.42/−0.90

The crystal structure is built up of bands of BO₄ tetrahedra, as well as planar BO₃-groups. The bands run alongside the crystallographic a -axis (see Figure 1). Three BO₄ tetrahedra form B₃O₉-rings, which are connected via two BO₃-groups to form “sechser”-rings alongside the ab plane. Additionally, the B₃O₉-rings are interconnected via two common corners to form four-membered rings (Figure 2). The B–O distances range from 1.421 to 1.555 Å within the BO₄ tetrahedra. The mean value of 1.474 Å corresponds very well with the average value of 1.476 Å reported by Zobetz [14]. The O–B–O angles lie in the rather wide range of 101.4–123.4°, which was also reported for the isotypic compounds β -Dy₂B₄O₉ [6] and β -Gd₂B₄O₉ [7]. The average value of 109.4° again is in good agreement with the reported value of 109.44° [14]. In the nearly planar BO₃-group ($\Sigma = 359.6^\circ$), the B–O bond lengths vary between 1.360 and 1.391 Å, while the O–B–O angles range from 114.9 to 122.7°. Both average values of 1.373 Å and 119.9° are in good agreement with the expected values, as the mean B–O distance for

planar as well as non-planar BO_3 -groups is 1.37 \AA [15] and the perfect angle in a planar BO_3 -group would be 120° . Similar results were found for $\beta\text{-Dy}_2\text{B}_4\text{O}_9$ [6] and $\beta\text{-Gd}_2\text{B}_4\text{O}_9$ [7] ($1.376 \text{ \AA}/119.9^\circ$). The positional parameters, as well as the B–O distances and the O–B–O angles can be found in Tables 2–4.

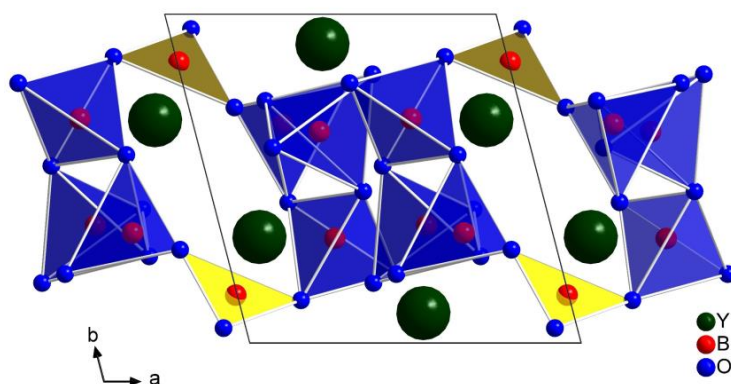


Figure 1. The interconnected BO_4 tetrahedra and BO_3 groups in $\beta\text{-Y}_2\text{B}_4\text{O}_9$ form bands along the a -axis.

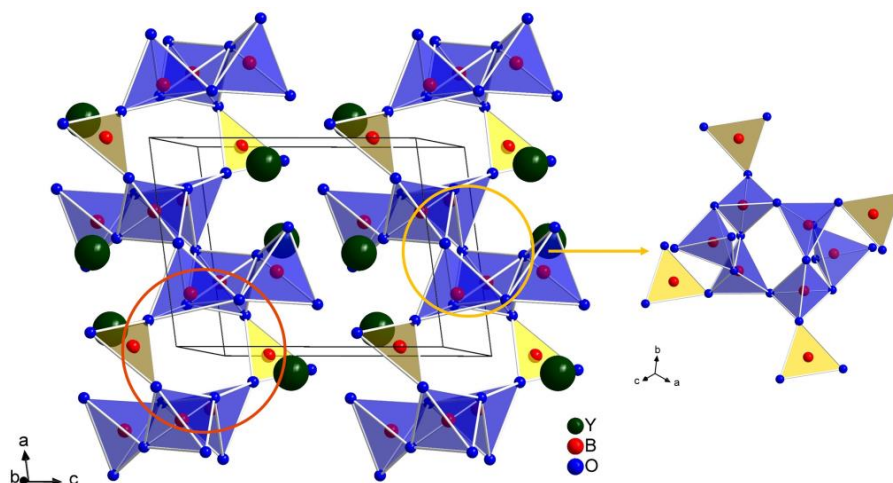


Figure 2. Crystal structure of $\beta\text{-Y}_2\text{B}_4\text{O}_9$ forming six-membered rings (one encircled in orange) and four-membered rings (one encircled in yellow and shown individually on the right).

Table 2. Atomic coordinates and equivalent isotropic displacement parameters $U_{\text{eq}}/\text{\AA}^2$. U_{eq} is defined as one third of the trace of the orthogonalized U_{ij} tensor (standard deviations in parentheses). All atoms are located on Wyckoff-site $2i$.

Atom	x	y	z	U_{eq}
Y1	0.8881(1)	0.6775(1)	0.3598(1)	0.0022(1)
Y2	0.5473(1)	0.0910(1)	0.2854(1)	0.0030(1)
B1	0.7321(3)	0.3347(3)	0.9806(2)	0.0052(2)
B2	0.6618(3)	0.6822(3)	0.9275(2)	0.0053(2)
B3	0.6255(3)	0.3572(3)	0.6505(2)	0.0056(2)
B4	0.0050(3)	0.8543(3)	0.8111(2)	0.0064(2)
O1	0.5040(2)	0.7902(2)	0.0204(2)	0.0057(2)
O2	0.4200(2)	0.1827(2)	0.5554(2)	0.0064(2)
O3	0.2360(2)	0.7364(2)	0.2113(2)	0.0060(2)
O4	0.7795(2)	0.4063(2)	0.5228(2)	0.0064(2)
O5	0.1375(2)	0.7163(2)	0.8570(2)	0.0069(2)
O6	0.5394(2)	0.5388(2)	0.7479(2)	0.0065(2)
O7	0.7741(2)	0.5720(2)	0.0412(2)	0.0058(2)
O8	0.8122(2)	0.8700(2)	0.8812(2)	0.0072(2)
O9	0.0677(2)	0.9547(2)	0.6761(2)	0.0077(2)

Table 3. Interatomic B–O distances/Å for β -Y₂B₄O₉ (standard deviations in parentheses).

Bond		Distance	Bond		Distance
B1	–O7	1.444(2)	B2	–O7	1.421(2)
	–O3	1.457(2)		–O6	1.457(2)
	–O1	1.497(2)		–O1	1.466(2)
	–O5	1.505(2)		–O8	1.483(2)
	∅	1.476		∅	1.457
B3	–O4	1.459(2)	B4	–O9	1.360(2)
	–O6	1.468(2)		–O8	1.367(2)
	–O2	1.474(2)		–O5	1.391(2)
	–O3	1.555(2)		∅	1.373
	∅	1.489			

Table 4. Bond angles/° for β -Y₂B₄O₉ (standard deviations in parentheses).

Bond		Angle	Bond		Angle
O1–B1–O5		101.4(2)	O1–B2–O8		101.7(2)
O7–B1–O5		101.7(2)	O6–B2–O8		104.9(2)
O3–B1–O1		104.0(2)	O6–B2–O1		108.3(2)
O7–B1–O3		111.6(2)	O7–B2–O1		112.6(2)
O7–B1–O1		114.9(2)	O7–B2–O6		113.6(2) 119.1(5)
O3–B1–O5		123.4(2)	O7–B2–O8		114.8(2)
∅		109.5	∅		109.3
O4–B3–O3		103.2(2)	O9–B4–O5		114.9(2)
O6–B3–O2		104.3(2)	O9–B4–O8		122.1(2)
O2–B3–O3		107.8(2)	O8–B4–O5		122.7(2)
O4–B3–O2		112.0(2)			
O6–B3–O3		112.0(2)			
O4–B3–O6		117.4(2)			
∅		109.5	∅		119.9

The Y³⁺ cations are located in the voids between the anionic borate bands. There are two crystallographically independent yttrium atoms in the structure: The first one is coordinated by nine oxygen atoms, the second one by ten oxygen atoms (see Figure 3). The Y–O distances lie in the range from 2.256 to 2.645 Å and are displayed in Table 5. This conforms to the reported values of β -Dy₂B₄O₉ (2.263–2.652 Å) and also to other high-pressure yttrium borates like β -Y(BO₂)₃ (2.383–2.419 Å) [3], α -Y₂B₄O₉ (2.401–2.602 Å) [4], and YB₇O₁₂ (2.308–2.659 Å) [5].

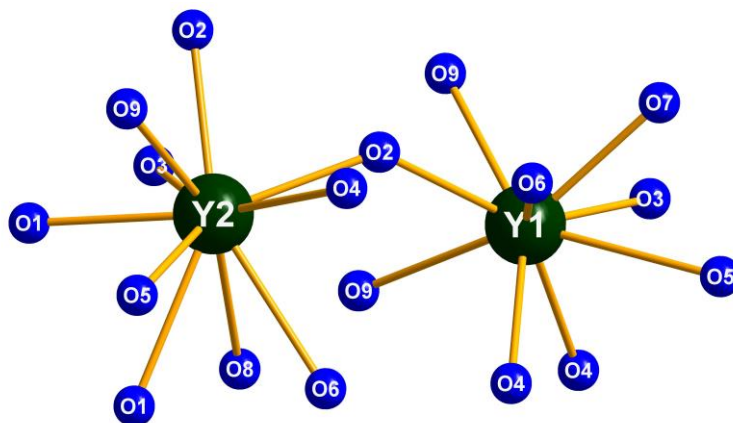
**Figure 3.** Coordination spheres of the two crystallographically independent yttrium sites in the crystal structure of β -Y₂B₄O₉.

Table 5. Interatomic Y–O distances/Å for β -Y₂B₄O₉ (standard deviations in parentheses).

Bond		Distance	Bond		Distance
Y1	–O7	2.299(2)	Y2	–O2	2.256(2)
	–O4	2.338(2)		–O2	2.351(2)
	–O4	2.359(2)		–O1	2.384(2)
	–O2	2.359(2)		–O4	2.414(2)
	–O9	2.390(2)		–O9	2.436(2)
	–O3	2.523(2)		–O8	2.487(2)
	–O9	2.573(2)		–O3	2.538(2)
	–O6	2.625(2)		–O5	2.541(2)
	–O5	2.645(2)		–O1	2.563(2)
				–O6	2.596(2)
	∅	2.457		∅	2.457

The charge distributions and bond valences were calculated using both the bond-length/bond-strength (BLBS; ΣV) [16,17], and the CHARDI concept (ΣQ) [18]. The results are shown in Table 6 and they are in good agreement with the expected values of +3 for yttrium and boron and –2 for oxygen.

Table 6. Charge distributions according to both, the bond-length/bond-strength (ΣV) and the CHARDI (ΣQ) concept.

Method	Y1	Y2	B1	B2	B3	B4				
ΣV	+2.92	+3.19	+3.02	+3.18	+2.92	+2.99				
ΣQ	+2.97	+3.01	+3.00	+2.97	+3.03	+3.03				
	O1	O2	O3	O4	O5	O6	O7	O8	O9	
ΣV	–2.09	–2.09	–1.90	–1.95	–2.07	–1.97	–2.16	–2.03	–1.94	
ΣQ	–1.98	–2.05	–1.86	–2.03	–1.99	–1.95	–2.18	–1.97	–1.99	

Further details of the crystal structure investigation may be obtained from The Cambridge Crystallographic Data Centre CCDC/FIZ Karlsruhe deposition service via www.ccdc.cam.ac.uk/structures on quoting the deposition number CCDC-1955299 for β -Y₂B₄O₉. The cif- and checkcif-files are also available in the Supplementary Materials.

2.2. Elemental Analysis

The semiquantitative EDX measurements were performed to prove the presence of europium in the β -Y₂B₄O₉ host. Figure 4 shows the resulting EDX spectrum, which clearly confirms that europium is present in the structure. The measured and averaged values from the measurements can be seen in Table 7. Additionally, small amounts of silicon were detected in three of the measurements, which most likely originates from the agate mortar that was used to homogenize the sample, which is well known for hard borates.

2.3. Photoluminescence Properties

The emission spectrum of a β -Y₂B₄O₉:Eu³⁺ (8%) single-crystal, obtained upon excitation by a blue laser diode ($\lambda_{exc} = 420$ nm) is shown in Figure 5. The Eu³⁺ transitions can be assigned to the ⁵D₀→⁷F_J (J = 0–4) transitions in the following way: the ⁵D₀→⁷F₀ transition corresponds to the single peak at 587 nm. The signals between 594 and 596 nm belong to the magnetic dipole transition (⁵D₀→⁷F₁), while the strongest bands in the spectrum from 610 to 623 nm can be assigned to the electric dipole transition (⁵D₀→⁷F₂). The ⁵D₀→⁷F₃ transitions occur as very weak signals in the range from 650 to 657 nm, and the signals between 684 and 705 nm belong to the ⁵D₀→⁷F₄ transitions [19]. The origin of the weak emission at 578–580 nm is the ⁵D₀→⁷F₁ transition, since 580 nm corresponds to an energy of

17.241 cm^{-1} . For the assignment of the transition, which matches the energy, the Dieke diagram was used [20].

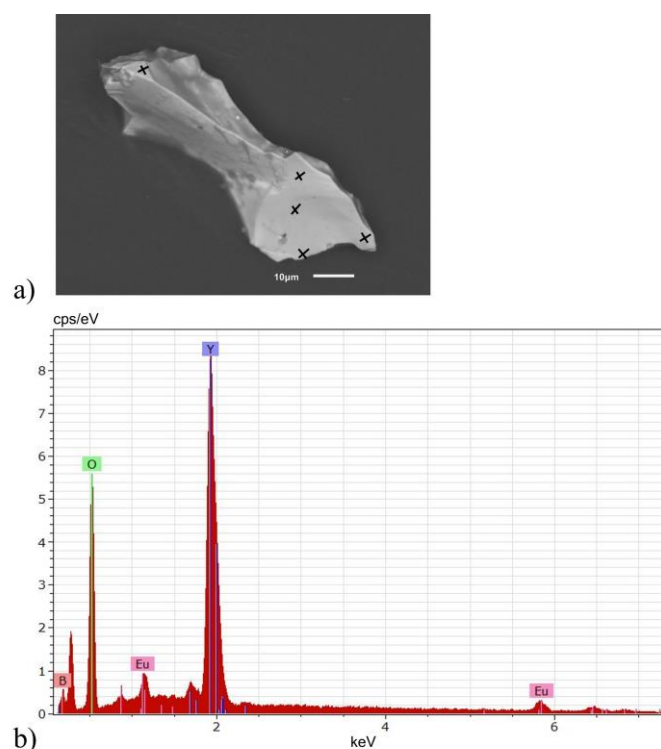


Figure 4. (a) Crystal used for the EDX measurement (crosses indicate the measured positions); (b) EDX spectrum of $\beta\text{-Y}_2\text{B}_4\text{O}_9\text{:Eu}^{3+}$ (8%). The unindexed peak at ~ 0.3 keV originates from carbon used for the sputtering process.

Table 7. Measured composition (normalized to 100%) of $\beta\text{-Y}_2\text{B}_4\text{O}_9\text{:Eu}^{3+}$ (8%) (wt %). Accuracy for all measured values $\pm 3\%$.

Element	Y	B	O	Eu	Si
M1	45.0	15.5	36.1	3.0	0.4
M2	41.2	13.0	33.2	12.5	0.1
M3	43.4	14.0	34.1	8.6	0.0
M4	42.1	15.3	34.9	7.7	0.1
M5	42.5	13.6	34.1	9.8	0.0
average	42.8(3)	14.3(2)	34.5(2)	8.3(7)	0.1
expected	46.1	11.7	38.9	3.3	

As can be seen in Figure 5, the so-called hypersensitive ${}^5\text{D}_0 \rightarrow {}^7\text{F}_2$ transition exhibits the strongest bands in the spectrum. For perfect inversion symmetry, e.g., for Eu^{3+} located onto a regular octahedral site, the intensity of the ${}^5\text{D}_0 \rightarrow {}^7\text{F}_2$ transition should be zero and thus the asymmetry ratio R should be zero too. However, since the ${}^5\text{D}_0 \rightarrow {}^7\text{F}_2$ transition is hypersensitive, any tiny distortion of the inversion symmetry will result in an increase of its intensity and thus in the R value. It is not uncommon that the ${}^5\text{D}_0 \rightarrow {}^7\text{F}_2$ transition is 10 times more intense than the ${}^5\text{D}_0 \rightarrow {}^7\text{F}_1$ transition. However, the correlation is not simple and correlating the luminescence color or symmetry ratio with a particular site symmetry or deviation from inversion symmetry is rather difficult.

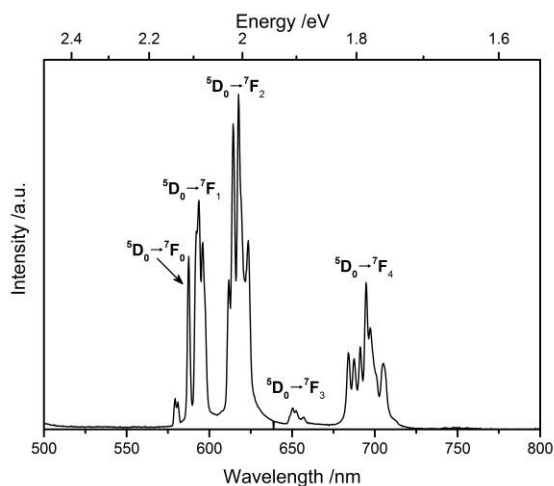


Figure 5. Emission spectrum of a β - $\text{Y}_2\text{B}_4\text{O}_9:\text{Eu}^{3+}$ (8%) single-crystal obtained upon excitation at 448 nm.

The factor R for the compound introduced in this paper has been calculated on the basis of the publication of K. Binnemans [19]. That leads to an integral of 9.4286 for the ${}^5\text{D}_0 \rightarrow {}^7\text{F}_2$ transition (604–635 nm) and to an integral of 1.8115 for the ${}^5\text{D}_0 \rightarrow {}^7\text{F}_1$ transition (589–604 nm). The R factor is calculated by $I({}^5\text{D}_0 \rightarrow {}^7\text{F}_2)/I({}^5\text{D}_0 \rightarrow {}^7\text{F}_1)$ and leads to $R = 5.2$.

3. Experimental Section

3.1. Synthesis

β - $\text{Y}_2\text{B}_4\text{O}_9$ was synthesized via a high-pressure/high-temperature experiment. For this synthesis, the starting materials Y_2O_3 (ChemPUR, Karlsruhe, Germany, 99.9%) and H_3BO_3 (Carl Roth, Karlsruhe, Germany, >99.8%) were ground together under ambient conditions in the stoichiometric ratio of 1:4.05, i.e., with a 5% excess of boric acid. The homogenized mixture was encapsulated in platinum foil, placed into a crucible made of α -BN and closed with a lid out of the same material (Henze Boron Nitride Products AG, Lauben, Germany). The crucible was placed into an 18/11 assembly, which was compressed and heated in a multianvil device based on a Walker-type module and a 1000 t downstroke press (both devices from Max Voggenreiter GmbH, Mainleus, Germany). A detailed description of the experimental setup can be found in the literature [21–23].

The sample was compressed to 7.5 GPa in 200 min, followed by a heating period of 10 min to 1673 K. This temperature was kept for 60 min, before the sample was slowly cooled down to room temperature in the following 240 min. Afterwards, the heating was switched off and the 600 min decompression process started. The recovered octahedral pressure medium was broken apart and the product carefully separated from the surrounding BN crucible and the platinum capsule. β - $\text{Y}_2\text{B}_4\text{O}_9$ could be obtained as colorless, irregular shaped crystals beside a significant amount of white microcrystalline powder.

The synthesis of the europium doped sample was carried out under the same conditions with Y_2O_3 , Eu_2O_3 (Smart Elements, Wien, Austria, 99.99%) and H_3BO_3 in the stoichiometric ratio of 0.46:0.04:2 as starting materials.

The X-ray powder diffraction data revealed that the reaction product is composed of β - $\text{Y}_2\text{B}_4\text{O}_9$ (about 59%) and π - YBO_3 as the main side phase. Attempts to synthesize a pure sample of β - $\text{Y}_2\text{B}_4\text{O}_9$ were not successful, π - YBO_3 always occurs as the main side product in the X-ray powder pattern.

3.2. Single-Crystal Structure Analysis

The intensity data of a β - $\text{Y}_2\text{B}_4\text{O}_9$ single-crystal was collected using a Bruker D8 Quest Kappa diffractometer equipped with a Photon 100 CMOS detector. An Incoatec microfocus X-ray tube in multilayer optics generated the monochromatized Mo $\text{K}\alpha$ radiation ($\lambda = 0.7107 \text{ \AA}$). A multiscan

absorption correction of the intensity data with SADABS 2014/5 [24] was applied on the data. For the structure solution and parameter refinement, the software SHELXS/L-2013 [25,26], as implemented in the program WINGX-2013.3 [27], was employed. No systematic extinctions were observed, which led to the only possible space groups $P1$ and $P\bar{1}$. During the refinement, the centrosymmetric space group was found to be correct, which is in agreement with the results from the isotopic compounds β -Dy₂B₄O₉ and β -Gd₂B₄O₉. All atoms could be refined with anisotropic displacement parameters.

3.3. Energy-Dispersive X-ray Spectroscopy (EDX)

A semiquantitative EDX measurement was performed in high vacuum on a Jeol JSM-6010LA scanning electron microscope (SEM) (Bruker, Billerica, MA, USA). The crystal was attached to a carbon tape and coated with carbon. The measurement was carried out under an acceleration voltage of 15 kV, a working distance of 14 mm, and a measurement time of 60 s. Five different spots on the crystal were selected, the measured chemical composition was averaged and normalized to 100%.

3.4. Luminescence Spectroscopy

The emission spectrum of a β -Y₂B₄O₉ single-crystal was collected using a setup equipped with an AvaSpec2048 spectrometer (AVANTES, Apeldoorn, Netherlands). A blue laser diode (THORLABS, Newton, MA, USA) with 448 nm wavelength was used as excitation source. Prior to the experiments, a spectral radiance calibration of the setup was carried out using a tungsten-halogen calibration lamp. The software AVA AvaSoft full version 7 was employed for data handling. The emission spectrum was measured in the range of 200–1100 nm and was background-corrected.

4. Conclusions

The new compound β -Y₂B₄O₉, which is isotopic to β -Dy₂B₄O₉ and β -Gd₂B₄O₉, was synthesized under the high-pressure/high-temperature conditions of 7.5 GPa and 1673 K using a Walker-type multianvil press. The structure was characterized via single-crystal X-ray analysis and it is built up of BO₃ groups as well as BO₄ tetrahedra, forming three-, four-, and six-membered rings.

The experiments to substitute yttrium with europium were successful, as proven by the EDX measurements of a β -Y₂B₄O₉:Eu³⁺ (8%) crystal. Thus, the luminescence properties of the europium-substituted sample were investigated. The emission spectrum shows typical Eu³⁺ photoluminescence with the strongest peak originating from the ⁵D₀→⁷F₂ electric dipole transition.

Supplementary Materials: The following are available online at <http://www.mdpi.com/2304-6740/7/11/136/s1>, the CIF and the checkCIF output files.

Author Contributions: Conceptualization, B.F. and H.H.; Validation, B.F., F.S. and G.H.; Formal Analysis, B.F., F.S. and G.H.; Investigation, F.S.; Writing—Original Draft Preparation, B.F.; Writing—Review & Editing, all authors; Supervision, T.J. and H.H.

Funding: This research received no external funding.

Acknowledgments: We thank M. Tribus for the EDX measurements and OSRAM Opto Semiconductors GmbH for the support in the investigation of the luminescence properties.

Conflicts of Interest: The authors declare no conflict of interest.

References

1. Levin, E.M.; Roth, R.S.; Martin, J.B. Polymorphism of ABO₃ type Rare Earth Borates. *Am. Mineral. J. Earth Planet. Mater.* **1961**, *46*, 1030–1055.
2. Lin, J.H.; Zhou, S.; Yang, L.Q.; Yao, G.Q.; Su, M.Z.; You, L.P. Structure and Luminescent Properties of Y_{17.33}(BO₃)₄(B₂O₅)₂O₁₆. *J. Solid State Chem.* **1997**, *134*, 158–163. [[CrossRef](#)]
3. Schmitt, M.K.; Huppertz, H. β -Y(BO₂)₃—A new member of the β -Ln(BO₂)₃ (Ln = Nd, Sm, Gd–Lu) structure family. *Z. Naturforsch. B* **2017**, *72*, 983–988. [[CrossRef](#)]

4. Schmitt, M.K.; Huppertz, H. High-pressure synthesis and crystal structure of α -Y₂B₄O₉. *Z. Naturforsch. B* **2017**, *72*, 977–982. [[CrossRef](#)]
5. Fuchs, B.; Schmitt, M.K.; Wurst, K.; Huppertz, H. High-Pressure Synthesis and Crystal Structure of the Highly Condensed Yttrium Borate YB₇O₁₂. *Eur. J. Inorg. Chem.* **2019**, *2019*, 271–276. [[CrossRef](#)]
6. Huppertz, H.; Altmannshofer, S.; Heymann, G. High-pressure preparation, crystal structure, and properties of the new rare-earth oxoborate β -Dy₂B₄O₉. *J. Solid State Chem.* **2003**, *170*, 320–329. [[CrossRef](#)]
7. Emme, H.; Huppertz, H. High-pressure synthesis of the new rare-earth oxoborate β -Gd₂B₄O₉. *Acta Crystallogr.* **2005**, *61*, i23–i24.
8. Lin, J.; Sheptyakov, D.; Wang, Y.; Allenspach, P. Structures and Phase Transition of Vaterite-Type Rare Earth Orthoborates: A Neutron Diffraction Study. *Chem. Mater.* **2004**, *16*, 2418–2424. [[CrossRef](#)]
9. Pitscheider, A.; Kaindl, R.; Oeckler, O.; Huppertz, H. The crystal structure of pi-ErBO₃: New single-crystal data for an old problem. *J. Solid State Chem.* **2011**, *184*, 149–153. [[CrossRef](#)]
10. Zhang, X.; Zhao, Z.; Zhang, X.; Marathe, A.; Cordes, D.B.; Weeks, B.; Chaudhuri, J. Tunable photoluminescence and energy transfer of YBO₃:Tb³⁺, Eu³⁺ for white light emitting diodes. *J. Mater. Chem.* **2013**, *1*, 7202–7207. [[CrossRef](#)]
11. Lokeswara Reddy, G.V.; Rama Moorthy, L.; Chengaiah, T.; Bungala Chinna, J. Multi-color emission tunability and energy transfer studies of YAl₃(BO₃)₄:Eu³⁺/Tb³⁺ phosphors. *Ceram. Int.* **2014**, *40*, 3399–3410. [[CrossRef](#)]
12. Lokeswara Reddy, G.V.; Rama Moorthy, L.; Packiyaraj, P.; Jamalaih, B.C. Optical characterization of YAl₃(BO₃)₄:Dy³⁺-Tm³⁺ phosphors under near UV excitation. *Opt. Mater.* **2013**, *35*, 2138–2145. [[CrossRef](#)]
13. Qi, Y.; Zhu, L.; Jiang, P.; Gao, W.; Cong, R.; Yang, T. Photoluminescence of complete solid solutions α -Y_{1-x}Eu_xB₅O₉ by sol-gel synthesis and thermal decomposition from Y_{1-x}Eu_x[B₆O₉(OH)₃]. *J. Solid State Chem.* **2019**, *277*, 731–737. [[CrossRef](#)]
14. Zobetz, E. Geometrische Größen und einfache Modellrechnungen für BO₄-Gruppen. *Z. Kristallogr.* **1990**, *191*, 45–57. [[CrossRef](#)]
15. Hawthorne, F.C.; Burns, P.C.; Grice, J.D. Boron: Mineralogy, Petrology, and Geochemistry. In *Reviews in Mineralogy*; Anovitz, L.M., Grew, E.S., Eds.; Mineralogical Society of America: Washington, DC, USA, 1996; Volume 33.
16. Brown, I.D.; Altermatt, D. Bond-Valence Parameters Obtained from a Systematic Analysis of the Inorganic Crystal Structure Database. *Acta Crystallogr.* **1985**, *41*, 244–247. [[CrossRef](#)]
17. Brese, N.E.; O’Keeffe, M. Bond-Valence Parameters for Solids. *Acta Crystallogr.* **1991**, *47*, 192–197. [[CrossRef](#)]
18. Hoppe, R.; Voigt, S.; Glaum, H.; Kissel, J.; Müller, H.P.; Bernet, K. A new route to charge distribution in ionic solids. *J. Less-Common Met.* **1989**, *156*, 105–122. [[CrossRef](#)]
19. Binnemanns, K. Interpretation of europium(III) spectra. *Coordin. Chem. Rev.* **2015**, *295*, 1–45. [[CrossRef](#)]
20. Dieke, G.H. *Spectra and Energy Levels of Rare Earth Ions in Crystals*; InterScience, Johan Wiley and Sons: New York, NY, USA, 1968.
21. Walker, D.; Carpenter, M.A.; Hitch, C.M. Some simplifications to multianvil devoces for high pressure experiments. *Am. Mineral.* **1990**, *75*, 1020–1028.
22. Walker, D. Lubrication, gasketing, and precision in multianvil exeriments. *Am. Mineral.* **1991**, *76*, 1092–1100.
23. Huppertz, H. Multianvil high-pressure/high-temperature synthesis in solid state chemistry. *Z. Kristallogr.* **2004**, *219*, 330–338. [[CrossRef](#)]
24. Sheldrick, G.M. *SADABS, v2014/5*; Bruker AXS Inc.: Madison, WI, USA, 2001.
25. Sheldrick, G.M. A short history of SHELX. *Acta Crystallogr.* **2008**, *64*, 112–122. [[CrossRef](#)] [[PubMed](#)]
26. Sheldrick, G.M. Crystal structure refinement with SHELX. *Acta Crystallogr.* **2015**, *71*, 3–8.
27. Farrugia, L.J. WinGX and ORTEP for Windows: An update. *J. Appl. Crystallogr.* **2012**, *45*, 849–854. [[CrossRef](#)]

